ORIGINAL ARTICLE

Impacts of Land-Use/Land-Cover Changes on Water-Borne Soil Erosion Using Geospatial Technologies and RUSLE Model over Chimbel Watershed of Upper Blue Nile Basin in Ethiopia

Abebe Senamaw[1] · **Temesgen Gashaw**[1] · **Muhammad Azhar Ehsan**[2]

Abstract

Land degradation in the form of soil erosion is one of the major environmental problems in the highlands of Ethiopia. This research was aimed to estimate the effects of changes in land use/land cover (LULC) on water-borne soil erosion in the Chimbel watershed of the Upper Blue Nile Basin, Ethiopia. The spatial and temporal LULC changes were analyzed using Landsat 5 TM 1989 and Landsat 8 OLI-TIRS 2019 images following a supervised classification technique with the Maximum-Likelihood Classification (MLC) algorithm. Soil erosion was estimated using the Revised Universal Soil Loss Equation (RUSLE) model. The result reveals that cultivated land and built-up area increased by 11.3 and 7%, respectively, while grassland (6.9%), forest (6.4%), bush/shrubland (4.9%), and water body (0.2%) were reduced between 1989 and 2019 periods. Consequently, the mean soil erosion rates estimated from the entire watershed were 24.0 t ha^{-1} year^{-1} in 1989 and 28.3 t ha^{-1} year^{-1} in 2019, which are higher than the tolerable soil loss (1–6 t ha^{-1} year^{-1}) and soil formation (10–14 t ha^{-1} year^{-1}) rates of the study region. Hence, applying a land management intervention to reverse the trend of LULC changes and thereafter its soil erosion is suggested for environmental improvement of the region.

Keywords Landsat · Land use/land cover · RUSLE · Water borne soil erosion

Abbreviations

LULC	Land use/land cover
ha	Hectare
yr	Year
t	Tone
RUSLE	Revised universal soil loss equation

✉ Abebe Senamaw
abebesenamaw@yahoo.com

Muhammad Azhar Ehsan
azhar@iri.columbia.edu

1   Department of Natural Resource Management, College of Agriculture and Environmental Science, Bahir Dar University, PO. Box: 5501, Bahir Dar, Ethiopia

2   International Research Institute for Climate and Society, Earth Institute at Columbia University, Palisades, NY, USA

1 Introduction

The highlands of Ethiopia are characterized as a region with a high rate of land degradation in general and soil erosion in particularly. According to the previous estimate, nearly 27 million hectares of the Ethiopian highlands were significantly eroded and over 2 million hectares of land was beyond reclamation (Hurni 1985). Meshesha et al. (2012) have also reported that the highlands of Ethiopia are heavily degraded, and it is frequently affected by drought and famine. In the Ethiopian highlands, approximately 1.5 billion tons of topsoil have been lost annually through soil erosion which can add about 1.5 million tons of grain to the country's annual harvest (Tamene and Vlek 2008). Crop production in the region is seriously affected by soil erosion and may lead to a complete failure of harvest on half of the cultivated land within the next few decades (Hurni 1985).

The rate and severity of soil erosion and land degradation partly depend on the land-use pattern (Woldemariam and Harka 2020). Continuous expansion of cultivated land at the expense of forest and shrubland is the major cause of land degradation and loss of soil fertility (Belayneh et al. 2019; Kidane et al. 2019). Changes in LULC from permanent

vegetation cover to the state of less vegetation cover have increased soil erosion (Bewket and Abebe 2013; Gashaw et al. 2019). Studies in different parts of the Ethiopian highland and in the Upper Blue Nile basin revealed that expansion of agricultural land into forest land is the major cause of land degradation in the form of soil erosion and is likely to have an impact in the future (Gebrehiwot et al. 2014; Tolessa et al. 2017).

In Ethiopia, there was a rapid rate of LULC changes, mainly expansion of cultivated land at the expense of forest land. For example, Gashaw et al. (2017) reported the expansion of cultivated land by 22.5%, while forest land was reduced by 45% from the year 1985–2015 in the Andassa watershed of the Upper Blue Nile basin. Kidane et al. (2019) in Guder watershed (highland of Ethiopia) also showed the expansion of cultivated land from 62% in 1973 to 67% in 2015, while forest land reduced from 14% in 1973 to 9% in 2015. Hence, the expansion of erosion-prone LULC types at expense of erosion resistance LULC classes exacerbates soil loss. The LULC changes have also contributed to physical and chemical changes in soil properties (Karltun et al. 2013).

Although several studies were undertaken in the highlands of Ethiopia on the impacts of LULC changes on the rate of soil erosion (Esa et al. 2018; Gashaw et al. 2017; Belayneh et al. 2019; Kidane et al. 2019; Moges and Bhat 2017; Tebebu et al. 2010), those studies were assessed only the changes in soil erosion rate and the areas covered under each soil erosion severity class due to the impacts of LULC changes. However, information about the changes from one erosion severity to another severity class (i.e., erosion severity change matrix) is important for abating the ongoing soil erosion rate in the Ethiopian highlands in general and in the study of watershed in particular. In addition, undertaking further research on a local scale is required for targeted intervention. This study was conducted in Chimbel watershed, which is a strategic location in Upper Blue Nile Basin of Ethiopia; it is one of the upper catchments of Lake Tana and the Grande Ethiopian Renaissance Dam (GRED). However, it experiences large-scale land degradation in the form of soil erosion which has a negative impact on large-scale water resource projects and agricultural products. To solve this problem, detailed studies about the impacts of LULC changes on soil erosion is necessary. Therefore, this study was aimed to assess the effects of LULC changes on soil erosion in the Chimbel watershed of the Upper Blue Nile Basin from the 1989–2019 period. The Revised Universal Soil Loss Equation (RUSLE) model was employed to provide estimates of annual soil erosion rate, in which most of the parameters were calibrated for the Ethiopian highland conditions (Hurni 1985) and applicable with the limited available data. The results of this study are necessary for land-use planners and decision-makers who require site-specific information on the magnitude of soil erosion and its spatial distribution to LULC changes. The information can be transferred to agricultural organizations, policymakers, land-use planners, and decision-makers. Thus, local communities can take appropriate measures to conserve vegetation, soil, and water in the watershed study and beyond.

2 Materials and Methods

2.1 Description of Study Area

Chimbel watershed is located between 11°33´–11°43´ N and 37º25´–37°32´ E (Fig. 1). It covers an area of 3705.1 ha, which is found within the Lake Tana sub-basin. It is one of the tributary river basins of the Upper Blue Nile Basin. Topographically, the watershed is dominated by high elevation, which ranges from 1769 to 2233 masl. The slope gradient of the watershed ranges from 0° to 46.2°. The upstream part is characterized by a mountain and highly dissected terrain with steep slopes, while the downstream part is characterized by gentle slope and flat area. The main rainfall season which accounts for around 70–90% of the annual rainfall occurs in the 4 months of June through September (Ehsan et al. 2021) with a mean annual rainfall of 1494–1451 mm and a mean maximum and minimum temperature of 26.6 °C and 15 °C, respectively. Moreover, the higher rainfall during boreal summer monsoon time, locally known as Kiremt, located in the northwestern highlands of Ethiopia is one of the main sources of water for the Blue Nile River of the River Nile. Agriculture is the dominant economic activity and the main source of livelihood for the population. The major crops grown in the watershed include maize (*Zea mays* L.), barley (*Hordeum vulgare*), teff (*Ergarostis teff* zucc), and Sorghum (*Sorghum bicolor*).

Chimbel watershed is endowed with diverse vegetation types due to topographic variation and located in highland of Ethiopia. Some of the indigenous vegetation types observed in study area include *Hagenia abyssinica* (kosso), *Cordia Africana* (Wanza), *Olea africana* (Weira), and *Ficus* spp (Warka). However, as confirmed from local communities, the coverage of these plant species has observed continuous reduction in a few decades mainly due to and changed to expansion of Eucalyptus plantation, cultivated land, and Chat plantation.

2.2 Image Pre-processing and Classification

In this study, Landsat collection 2 level 1 Landsat 5 Thematic Mapper (TM) collection 2 level 1 (Landsat 4-5TM C2 L1) 1989 and Landsat 8 Operational Land Imager (OLI) and Thermal Infrared Sensor (TIRS) collection 2 level 1 (Landsat 8OLI/TIRS C2 L1) 2019 with a resolution of 30 m were used for developing the LULC maps of the study watershed.
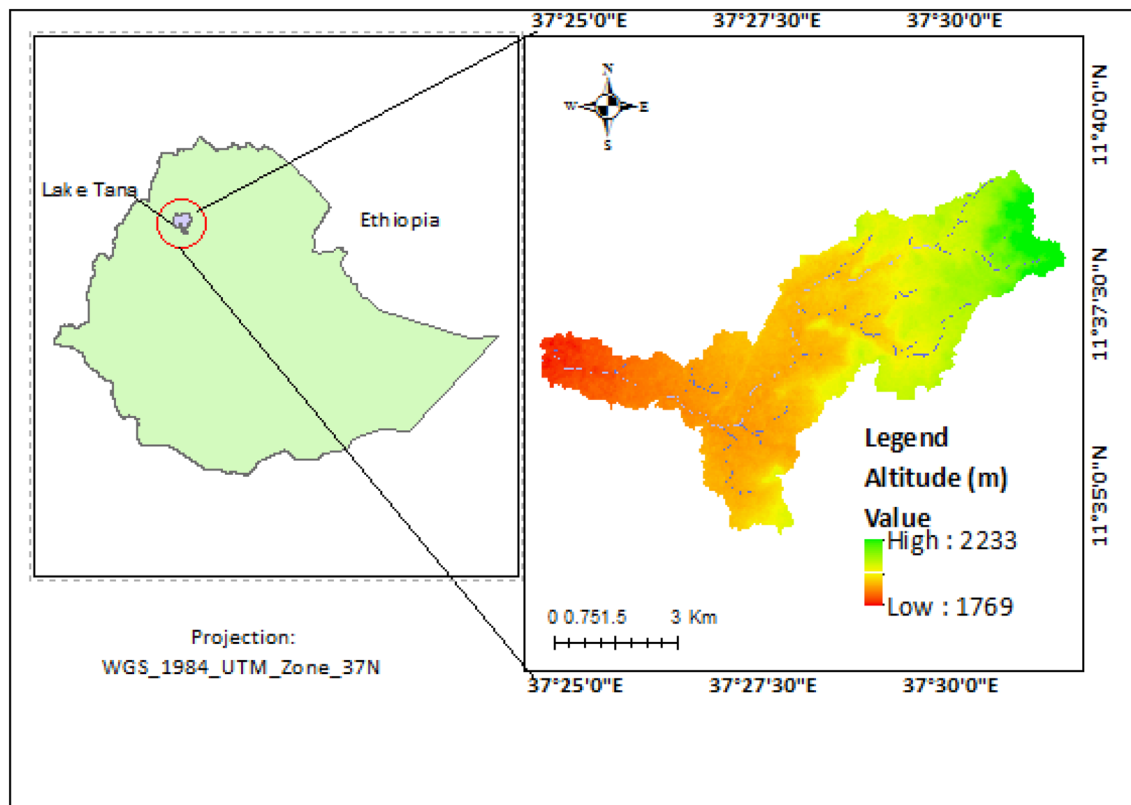
Fig. 1 Location map of the study watershed

The images are obtained from path 170 and raw 052, and have 30 m grid spatial resolution. The February and March month images were downloaded for Landsat 5 TM 1989 and Landsat 8 OLI-TIRS 2019, respectively, and hence, the seasonal variation of the two Landsat images narrowed. Digital image data files were downloaded in zipped files from the United States Geological Survey (USGS) website (https://earthexplorer.usgs.gov/). Both satellite images were in TIFF form. Satellite images were corrected for atmospheric, sensor, and illumination variance sources through radiometric corrections like haze reduction; noise reduction and finally histogram equalization (histogram equalization and nose/haze reduction). The images were geo-referenced into the same map projection of World Geodetic System 1984 Zone 37. Image classifications were made following a supervised classification technique with the Maximum-Likelihood Classification (MLC) algorithm by collecting ground control points from the five major LULC classes (Table 1).

Unlike unsupervised image classification, supervised image classification is mainly controlled by the analyst that selects the pixels that are representative of the desired area. In supervised image classification which gives the best result, training data were involved, while in unsupervised image classification involves algorithms to examine the unknown pixels in an image and assign them into a number of class based on natural groupings or clusters present

Table 1 Descriptions of the LULC categories identified in the study watershed

LULC class	Description
Forest land	Areas covered with dense tress; both natural indigenous tree and riverine vegetation species; which includes *Eucalyptus* plantations
Bush/shrub land	Land covered by small trees, bushes, and shrubs in some cases mixed with grasses; less dense than forests
Cultivated land	Areas used for perennial and annual crops and irrigated sites
Water body	Areas with open water such as ponds, lakes, streams, rivers, and reservoirs
Grassland	All areas covered with grass and used for animal grazing
Built-up areas	Settlement areas (towns, construction sites, and cluster and dense rural settlements)

in the image (Lillesand and Kiefer 1979). Before executing supervised image classification for each predetermined land-use/land-cover class, training samples were selected by delimiting polygon around representative sites. Gao and Liu (2010) reported that a satisfactory spectral signature is the one ensuring that there is minimal confusion among the land use/land covers to be mapped. Information from field data and prior 1989 was utilized to identify training area representing each land-use/land-cover class.

After image classification, the accuracy of the LULC maps was executed using an error matrix (Foody 2002; Zhu and Woodcock 2014; Shalaby and Tateishi 2007). It is performed by comparing a classified image with a reference map based on different sources of information. (e.g., field surveys, Google Earth, and original mosaic maps). The reference points for the 2019 period were collected from field surveying using Global Positioning System (GPS) and high-resolution Google Earth Image, while for the year 1989, reference points were composed of Google Earth Image and original mosaic images. The accuracy of classification was evaluated with error (confusion) matrix and kappa coefficient using GPS field collected points and image of Google Earth.

Besides, the number of conversions from one LULC to another LULC category within the study periods (i.e., transition matrix) was done using ArcGIS10.2 and ERDAS Imagine 2014 software. The result was a two-way cross matrix indicating a different combination of "from-to" change classes which was used to describe the main types of changes undertaken during the 1989 and 2019 periods. The rate of each LULC class was calculated using Eq. 1

$$G = \frac{R - P}{T}, \qquad (1)$$

where G is the rate of LULC changes (ha), R is the recent area of LULC (ha), P is the previous area of LULC (ha), and T is the time interval between R and P in years.

Parameterization of the RUSLE model The Revised Universal Soil Loss Equation (RUSLE) is an empirical erosion model recognized as standard method to calculate the average risk of erosion on arable land (Prasannakumar et al. 2012; Benavidez et al. 2018; Mirakhorlo and Rahimzadegan 2020). The model provides a rather and yet comprehensive framework for assessing soil erosion and its causative factors (Alexakis et al. 2013; Kalambukattu and Kumar 2017; Phinzi and Ngetar 2019). It is a combination of empirical and process-based routines designed to make optimum use of the database on which the USLE was anchored. RUSLE considers rainfall (*R*), soil erodibility (*K*), cover management (*C*), topography (*LS*), and cover management (*P*) as important factors affecting soil erosion.

In this study, soil erosion was estimated using the RUSLE model (Wischmeier and Smith 1978), which computes the long-term mean annual soil loss rate using five factors as described in Eq. 2

$$A = R \times K \times \mathrm{LS} \times C \times P, \qquad (2)$$

where A is the annual soil erosion rate (t ha^{-1} year^{-1}), R is the rainfall erosivity factor (MJ mm ha^{-1} h^{-1} year^{-1}), K is the soil erodibility factor (t ha h ha^{-1} MJ^{-1} mm^{-1}), LS is the topographic factor which includes the slope length and steepness factors (Dimensionless), C is the LULC factor (Dimensionless), and P is the land management practice factor (Dimensionless).

Rainfall erosivity (R) factor Calculation of the R factor requires rainfall intensity data, which represents the strength of the rainfall and it is associated with the rate and amount of runoff, which have the potential to cause erosion (Arnoldus et al. 1980). Due to the absence of rainfall intensity data in the watershed, the R factor in this study was developed using the regression equation established by Hurni (1985) for the Ethiopian conditions (Eq. 3). Hence, the R factor was calculated from the mean annual rainfall data of four meteorological stations for the periods 1989–2019 (Table 2), which were obtained from the National Meteorological Service Agency (NMSA). These data were interpolated using the Inverse Distance Weighted (IDW) interpolation technique. The R factor analyzed was found in the range of 807.4–831.6 MJ mm h^{-1} ha^{-1} year^{-1} (Fig. 2a)

$$R = (0.562 \times P) - 8.12, \qquad (3)$$

where R is the rainfall erosivity factor (MJ mm h^{-1} ha^{-1} year^{-1}) and P is mean annual rainfall (mm).

Table 2: List of meteorological stations and their corresponding mean annual rainfall during 1989–2019 periods.

Soil erodibility (K) factor The erodibility of soil is an expression of its inherent resistance of soil particles to detach and transport by rainfall runoff. K factor is an essential component for predicting soil erosion using the RUSLE model (Wolka et al. 2015). The K factor map of this study was developed (Fig. 2b) following Eq. 4 (Wischmeier and Smith 1978) using the soil physical (clay, silt, and sand) and chemical properties (organic matter content) data of the

Table 2 List of meteorological stations and their corresponding mean annual rainfall during 1989–2019 periods

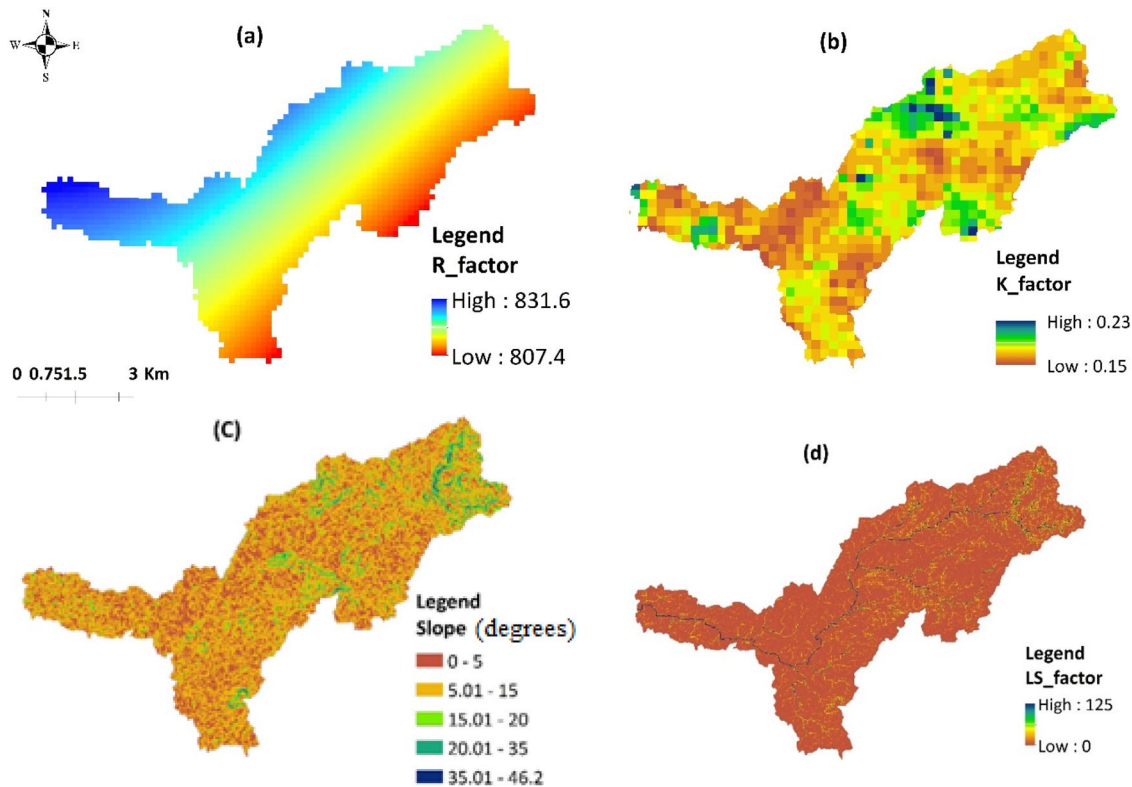| Stations	Latitude	Longitude	Elevation (m a.s.l)	Mean annual rainfall (mm)	R factor
Bahir Dar	11.60	37.32	1827	1428	794.4
Deke-Esti-fanos	11.90	37.27	1802	1578	878.7
Tis Abay	11.49	37.58	2642	1361	756.8
Zege	11.71	37.32	1808	1618	901.2

Fig. 2 The *R* factor (**a**), *K* factor (**b**), slope gradient (**c**), and LS factor (**d**) maps of the study watershed

upper layer (0–30 cm), which was accessed from the international soil reference information center (ISRIC) database (Hengl et al. 2017). The obtained data from ISRIC have a spatial resolution of 250 m

$$K = \left[2.1 \times M^{1.14} \times 10^{-4} \times (12 - SOM) + 3.25 \times (S - 2) + 2.5(P - 3)\right]\big/100, \tag{4}$$

where *K* is the soil erodibility factor; SOM is the soil organic matter content; *S* and *P* are soil structure and permeability codes, respectively; M is a newly defined term, that is $M = (\%silt + \%ery\ fine\ sand) \times (100 - \%clay)$.

Topographic (LS) factor The LS factor represents the combined effects of the slope length (L factor) and slope steepness (S factor) factors on water-induced soil erosion. The LS map of this study was developed using Eq. 5 (Moore and Burch 1986) using the Shuttle Radar Topographic Mission (SRTM) Digital Elevation Model (DEM), which has a resolution of 30 m. The SRTM data were accessed from the USGS website (https://ers.cr.usgs.gov)

the weight for all cells that flow into each downslope cell; cell size is the length of cell sides; L and S stand for slope length and steepness factors; the slope is the slope gradient in degrees. The LS factor and slope maps of the study area are indicated in Fig. 2c, d.

Cover management (C) factor The cover management factor describes how each land cover (e.g., forest, cropland, grassland, and bushland) affects the rate of soil erosion (Wischmeier and Smith 1978). To develop *C* factor maps of the 1989 and 2019 periods, corresponding *C* values were assigned for each LULC type based on an intensive review of previous studies in the study region (Gashaw et al. 2019, 2020; Moges and Bhat 2017; Haregeweyn et al. 2017) (Table 3 and Fig. 3).

Conservation practice (P) factor The P factor refers to management practices such as mulching, terracing, strip

$$LS = (fac \times cell\ size/22.13)^{0.4} \times \left(0.01745 \sin\left(slope/0.0896\right)\right)^{1.4} \times 0.4, \tag{5}$$

where fac (flow accumulation) is a raster-based total of accumulated flow to each cell as determined by accumulating

cropping, contour tillage, and other protection measures and their effect in reducing the amount and rate of water-induced

Table 3 The assigned *C* and *P* factor values for the corresponding LULC types in this study compiled from published sources

LULC class	C factor	P factor
Cultivated land	0.15	0.9
Grassland	0.01	0.8
Bush/shrub land	0.014	0.8
Water body	0.0	0.0
Forestland	0.001	0.7
Built-up area	0.05	0.9

soil erosion (Demirci and Karaburun 2012). P values can be determined by considering the type of conservation measures implemented in the study area. However, as confirmed from intensive field observations, there are no significant soil and water conservation practices implemented in this watershed, and for that matter, in the Ethiopian Highlands (Hurni 1983). As a result, *P* factor values were assigned to each LULC types from preceding studies in the highland regions (Table 3; Fig. 4). As shown in Fig. 4, the *P* values ranges from 0.0 to 0.9, in which the highest value is assigned to areas which area vulnerable to erosion.

2.3 Methods of assessing effects of LULC changes on soil losses

The mean annual soil loss rate of the study watershed was estimated by multiplying the five RUSLE factors in the Arc-GIS 10.2 raster calculator tool. To comprehend the effects of LULC changes on soil erosion, *P* and *C* factors are changed and other RUSLE parameters are kept constant. However, all the RUSLE model parameters were initially converted into the uniform coordinate system (UTM Zone 37 N using the WGS 1984 datum) and grid cell size (i.e., 30 m). For analysis of soil loss associated with LULC change, each raster dataset was converted into polygon and Zonal statistics. To quantify soil erosion class changes between the 1989 and 2019 periods, the conversion matrix was calculated.

3 Results and discussion

3.1 LULC changes between 1989 and 2019

The accuracy assessment result reveals that the overall accuracy of 92.67 and 90.19% and a Kappa coefficient of 0.90 and 0.80 for the LULC maps of 1989 and 2019 periods, respectively, were attained. The obtained overall classification accuracy and Kappa statics are above the recommended values (Foody 2010). Similarly, classification accuracy for each land use/land cover was also executed (Table 4). The resulting of classification accuracy of LULC in two periods

was reasonably good and accepted for the subsequent change analysis and change detection. Thus, this classification is feasible for further application.

Among the LULC types, cultivated land occupies the largest share of the total area (43.3% in 1989 and 54.6% in 2019) followed by grassland and bush/shrubland. While water bodies occupy the smallest portion, which account for about 0.4 and 0.2% in 1989 and 2019 periods, respectively (Table 5 and Fig. 3). The change detection result between the 1989–2019 periods showed that cultivated and built-up areas have increased by 418.8 ha (11.3%) and 257.5 ha (7%), respectively. While water body, grassland, bush/shrub, and forest land were reduced by 0.2, 6.9, 4.9, and 6.4%, respectively. The result shows that there is an expansion of built-up and cultivated land at the expense of natural vegetation covers. This is consistent with the finding (Aneseyee et al. 2020) which showed that there is an expansion of cultivated and built-up area at the expense of forest, grazing, and shrubland in the Winike watershed (Omo Gibe basin Ethiopia). Similarly, Garede and Minale (2014) stated that there was a continued expansion of cultivated land and settlement from the period of 1973–2011 which has brought a significant decrease in the water bodies, forests, and bushlands in the Ribb watershed in Northwestern Ethiopia. In contrast, Mekuriaw (2017) states that cropland decreased by 9%, while grassland and vegetation cover increased by 136% and 96% from the period of 2010–2015 in Melaka watershed, in the highlands of Ethiopia. Gashaw et al. (2019) have also indicated that the expansion of cultivated land and built-up areas is at the expense of forest, shrubland, and grasslands in the Andassa watershed (Northwestern Ethiopia) between the 1985 and 2015 periods.

The transitions of each LULC type between 1989and 2019 were also assessed (Table 6; Fig. 5). The diagonals of the matrix in Table 6 are the unchanged LULC area, while the off-diagonals are the transitions from one LULC to another. The result reveals that 179, 46.3, 16.7, and 325 ha of bush/shrubland were converted to grassland, built-up area, forestland, and cultivated land, respectively. Although a significant area of bush/shrubland was lost to other land-use categories, 163.4, 4.6, 81.5, and 136.4 ha of land were gained from grassland, built-up area, forest land, and cultivated land, respectively. Similarly, 325.6, 494.2, 57.1, 106.1 and 1.3 ha of cultivated land were converted from bush/shrubland, grassland, built-up area, forest land, and water body, respectively. While 136.4, 226.3, 186.9, and 16 ha of cultivated land were converted to bush/shrubland, grassland, built-up area, and forest land, respectively. During this time, built-up gained 46.3, 73, 17.4, and 187 ha of land from bush/shrubland, grassland, forestland, and cultivated land, respectively. In reverse, some portion of the built-up area was converted to other land-use categories. For example, bush/shrubland (4.6 ha), grassland (4.6 ha), forestland
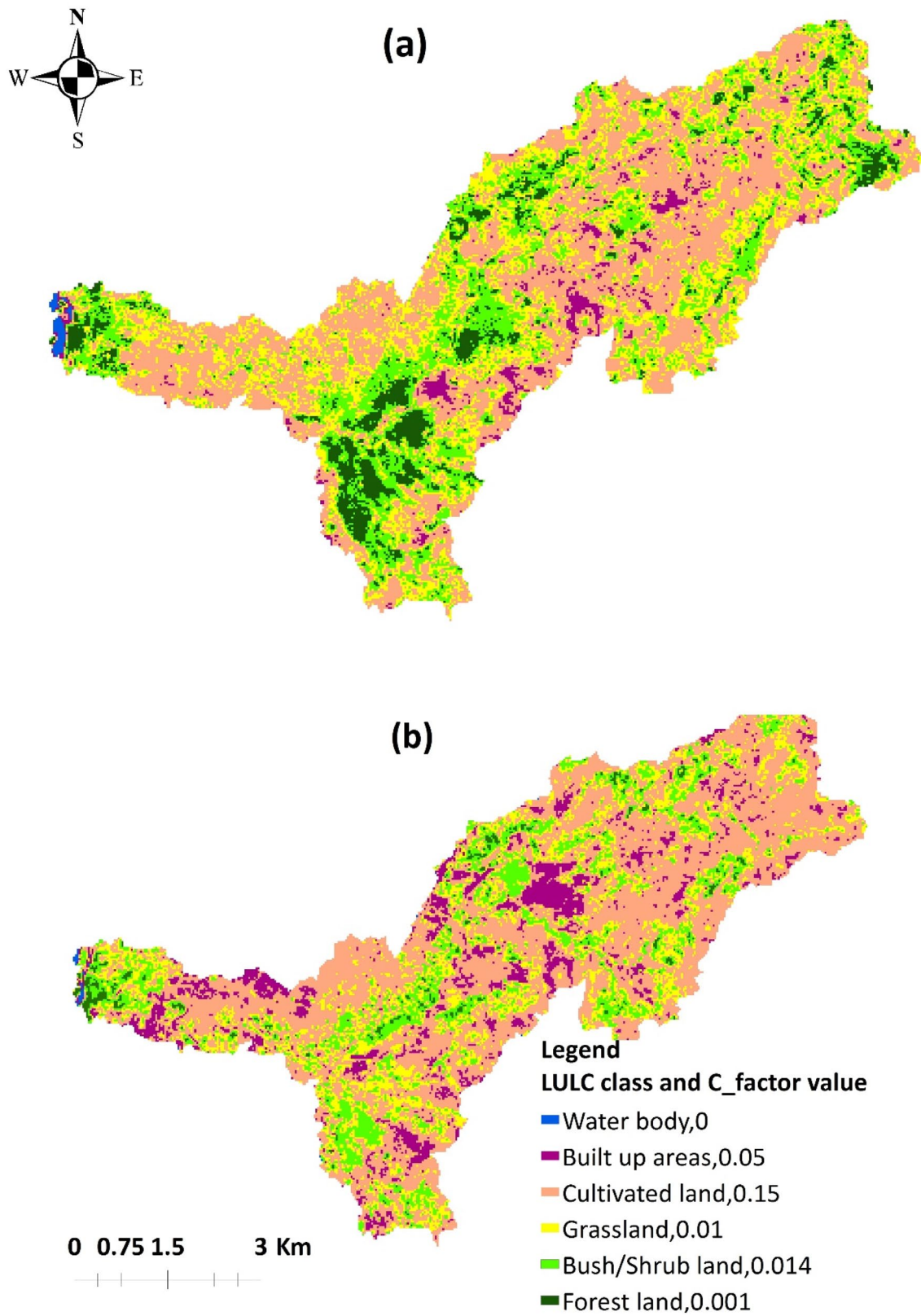
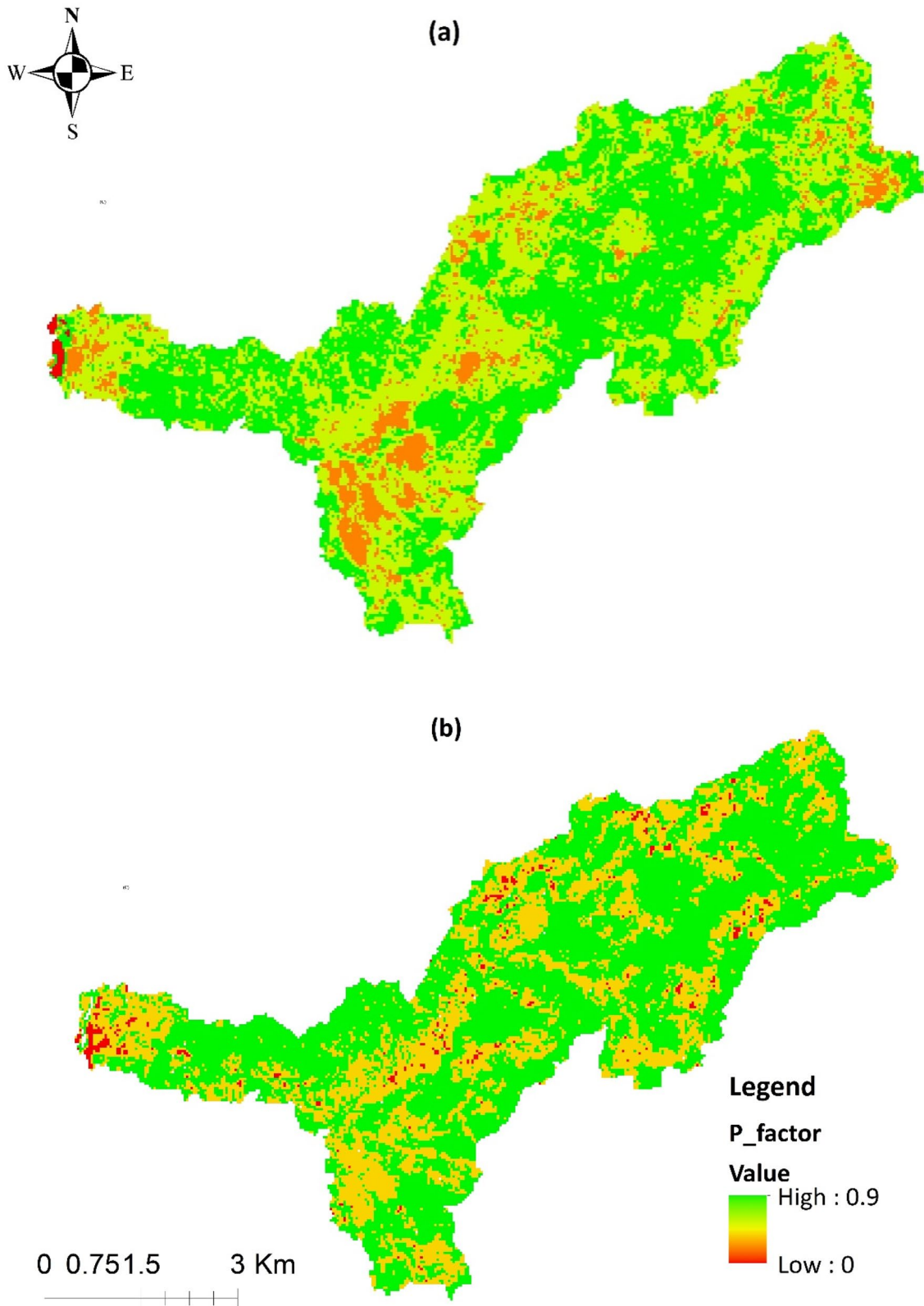**Fig. 3** The 1989 (**a**) and 2019 (**b**) LULC and C factor maps of the study area

Fig. 4 The 1989 (**a**) and 2019 (**b**) P factor maps of the study area (the highest value is assigned to areas which is vulnerable to erosion)

Table 4 The accuracy assessment results of the 1989 and 2019 period LULC maps

LULC class	1989			2019		
	Producers' accuracy (%)	Users' accuracy (%)	Conditional kappa	Producers' accuracy (%)	Users' accuracy (%)	Conditional kappa
Bush/shrub land	91.4	93.0	0.9	84.6	78.6	0.8
Grassland	91.7	94.3	0.9	96.2	91.5	0.7
Built-up area	100.0	100.0	1	75	75	1.0
Cultivated land	92.65	90.0	0.9	84.2	84.2	0.8
Water body	100.0	100.0	1	100.0	100.0	1.0
Forestland	95.7	94.3	0.9	75.4	87.8	0.9
Overall accuracy	92.7%			90.2%		
Kappa coefficient	90.3%			80.1%		

Table 5 The area coverage of LULC classes and rate of changes in study area between 1989 and 2019

LULC class	1989		2019		Rate of change (ha year⁻¹)
	Area (ha)	%	Area (ha)	%	
Bush/shrub land	709.0	19.1	529.2	14.3	− 6.0
Grassland	969.1	26.2	715.0	19.3	− 8.5
Built-up area	108.9	2.9	366.5	9.9	8.6
Forest land	299.7	8.1	64.3	1.7	− 7.8
Cultivated land	1603.8	43.3	2022.6	54.6	14.0
Water body	14.5	0.4	7.6	0.2	− 0.2
Total	3705.1	100.0	3705.1	100.0	

(1.2 ha), and cultivated land (57.1 ha) were gained from built-up areas. As shown in Table 6. Although it was a small proportion 1.8, 0.9, 2.1, 1.5, and 1.3 ha of water body was converted to bush/shrubland, grassland, built-up area, forest land, and cultivated land, respectively.

The finding of this study reveals a large proportion of bush/shrubland; grassland and forest land were converted to cultivated land. This result was consistent with the findings

of other studies conducted in different parts of the country. For instance, Gashaw et al. (2020) in Andassa watershed, Belay and Mengistu (2019) in Muga watershed; Teferi et al. (2013) in Jedeb watershed, the upper Blue Nile basin in Ethiopia reported the conversion of shrubland, grassland, and forest land to cultivated land. Similarly, a considerable area of cultivated land was converted to built-up areas (Table 6 and Fig. 5).

Expansion of built-up areas was due to population growth in association with the expansion of Bahir Dar town which was founded close to the study area. This result is in agreement with the finding of Kidane et al. (2019) who reported the high rate of soil erosion due to vegetation degradation in the Guder watershed. Gashaw et al. (2019) in the Andassa watershed have also described the increase of soil erosion and sediment yield losses between 1985 and 2015 periods as a result of reductions of erosion-resistant LULC types and expansion of erosion vulnerable LULC types (i.e., cultivated land). The results of this study are also aligned with the findings of Moges and Bhat (2017) in the Rib watershed, which reported the intensification of mean annual soil erosion rates between 1986 and 2016 periods due to the expansion of cultivated land and diminish of vegetation covers.

Table 6 The LULC change matrix between 1989 and 2019 periods (area in ha)

1989	2019						Total area	Loss
	BSL	GL	BU	FL	CL	WB		
BSL	**141.5**	178.9	46.3	16.7	325.6		709.0	567.5
GL	163.4	**220.9**	73.0	17.6	494.2		969.1	748.2
BU	4.6	4.6	**40.7**	1.2	57.1	0.8	108.9	68.2
FL	81.5	83.4	17.4	**11.3**	106.1		299.7	288.4
CL	136.4	226.3	186.9	16.0	**1038.2**		1603.8	565.6
WB	1.8	0.9	2.1	1.5	1.3	**6.8**	14.5	7.7
Total area	529.2	715.0	366.5	64.3	2022.6	7.6	3705.1	
Gain	387.7	494.1	325.7	53.0	984.3	0.8		

BSL bush/shrub land, *GL* Grassland, *BU* built-up area, *Fl* forest land, *CL* cultivated land, *WB* water body

The bold diagonal values are indicating the unchanged land use/land cover and soil erosion respectively
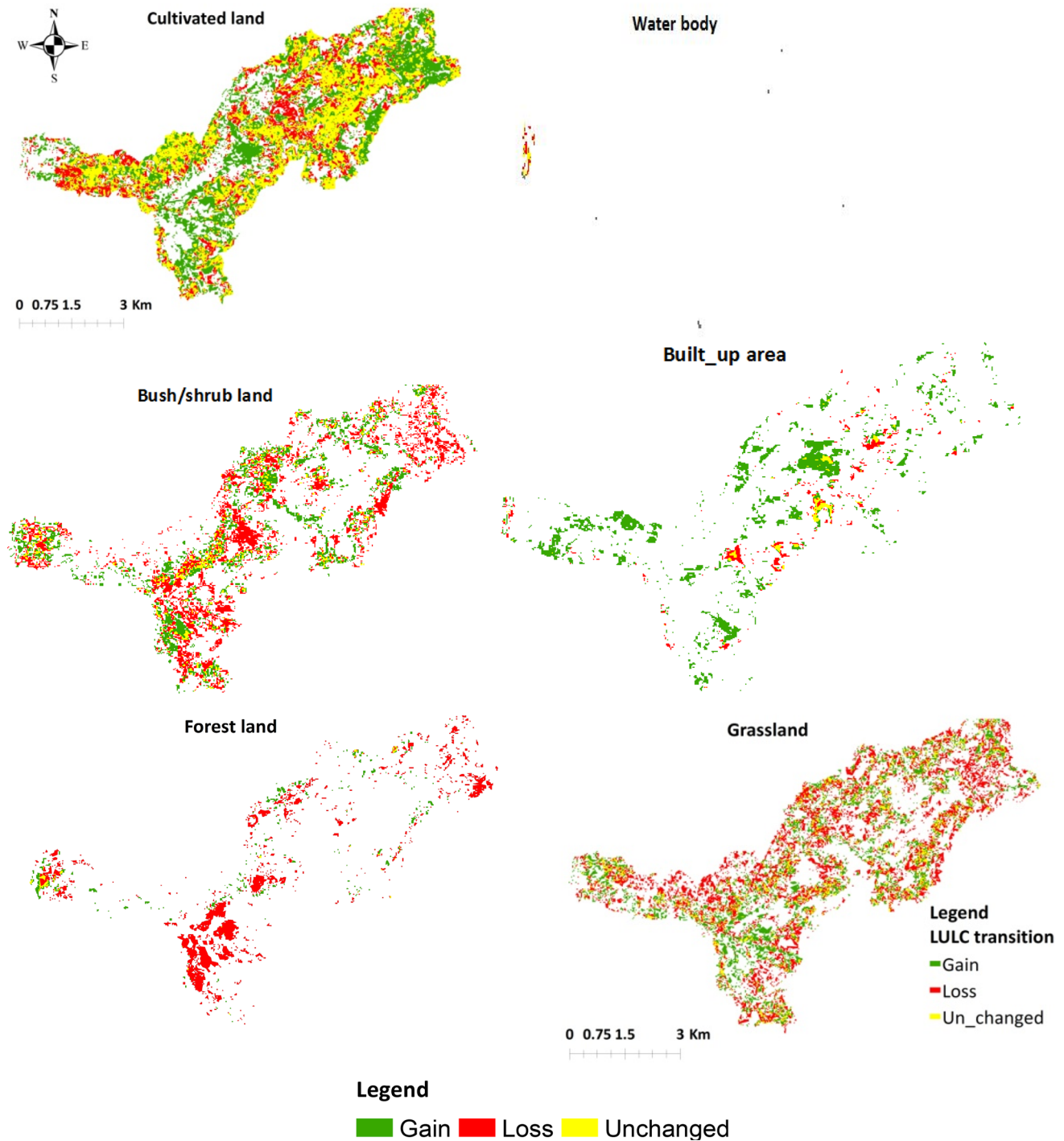
Fig. 5 The gain, loss, and unchanged areas of each LULC types in the Chimbel watershed between 1989 and 2019 periods

Effects of LULC changes on soil losses This study used (Kidane et al. 2019; Negese 2021; Zerihun et al. 2018; Haregeweyn et al. 2017) soil erosion severity categories to effectively visualize the spatial distribution of soil erosion hotspot areas and the results are presented in Fig. 6 and Table 7. The result showed that about 47% of the study area in 1989 was under very slight erosion risk class, while the remaining areas were under slight-to-very severe erosion risk classes. In 2019, 46.8% of the study area was affected by very slight erosion risk, while 23% of the area was covered by a very severe erosion risk class. There was an increasing trend in moderate and very severe erosion risk as compared to the year 1989, while very slight and slight erosion risk shows a decreased trend (Fig. 6 and Table 7).
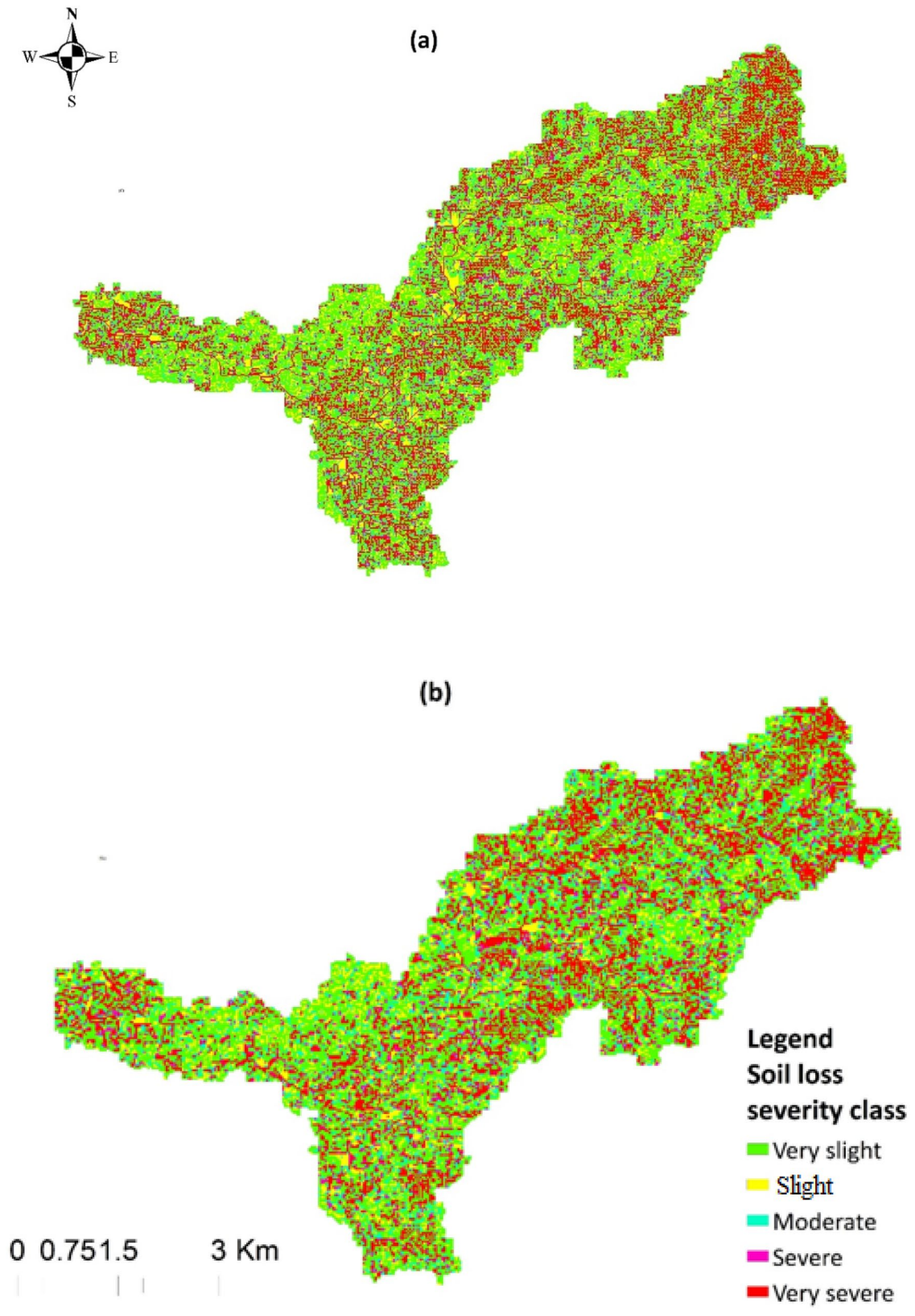
Fig. 6 The estimated mean annual soil loss rates of the study watershed in 1989 (**a**) and 2019 (**b**) periods

Table 7 The area coverage and amount of soil losses for each severity classes. Adopted from Haregeweyn et al. (2017)

Soil loss (t ha^{-1} year^{-1})	Severity classes	1989 (ha)	1989 (%)	2019 (ha)	2019 (%)	Total soil loss (t year^{-1}) 1989	Total soil loss (t year^{-1}) 2019
< 5	Very slight	1747	47.2	1704.3	46	4566.2	5236
5_15	Slight	467	12.6	399.4	10.8	5190.8	5504.1
15–30	Moderate	314.7	8.5	379.6	10.2	7872.5	10,562.9
30–50	Sever	407.4	11	393.2	10.6	17,018.5	11,833.4
> 50	Very sever	768.9	20.8	828.6	22.4	55,939.2	71,786.9
Total	–	3705.1	100	3705.1	100	90,587.3	104,923.2

The spatial distribution of soil erosion shows that severe and very severe soil erosion affected areas are mainly found in upper and steeper areas and the lowest was mostly found in gentle slopes (Fig. 6). The severity of erosion was significantly higher on areas where vegetation cover was converted to non-vegetated areas, areas with high drainage density coupled with steep slope topography in study periods (Fig. 6). Mekuriaw (2017) found high soil erosion in areas where there are sparse vegetation cover and poor soil conservation measures. Based on the finding, moderate, severe, and very severe erosion class as an indicator of land degradation occurred in the study area. As confirmed from field observation, there is severe soil erosion like gullies and rill erosion. However, there is little biological conservation measure at different scales which were conducted by local community participation. Within this intervention, there is a continued forest clearance and cultivation of steep slopes to support the demand of the rapid population growth which aggravates the problem at large. Expansion of cultivated land at expense of natural vegetation has intensified the problem of land degradation through soil erosion by water (Bewket and Abebe 2013).

The transition between each soil severity class was analyzed and the results are presented in Table 8. As shown in Table 8, about 170 ha and 190 ha of land were converted from very slight-to-moderate and very severe erosion class, respectively, from the year 1989–2019 which is an indicator for expansion erosion-prone areas. As shown in Table 8, 125.1, 107.5, 92.8, and 190.4 ha of very slight erosion

severity class were converted to slight, moderate, severe, and very severe erosion severity class. While 132.2, 76.2, 97.6, and 168.2 ha of soil severity class were converted from slight, moderately severe, and very severe soil erosion class to very slight erosion class, respectively. This implies that there is net losses of 42.7 ha of very slight erosion severity class were converted to other. Similarly, 61.4,67 and 66 ha of land were converted from slight to moderate, severe, and very severe erosion severity classes, respectively. The transition from 828.5 ha very severe erosion severity class was the result of the transition from very slight (190.4 ha), slight (66.4 ha), moderate (62.2 ha), and severe (105.5 ha) erosion severity class. In this case, very severe erosion severity class gain, 59.6 ha of land compared to a net loss to other severity class. Increased in severe and very severe erosion risk is mainly due to LULC transition which results from diminished erosion resistance areas (vegetation cover) and increased erosion-prone LULC types like cultivated land (Fenta et al. 2016; Esa et al. 2018). Besides, the area under different soil severity classes that remained unchanged was estimated at 1231.2, 141.2, and 97.4 ha in case of very slight, slight, moderate, severe, and very severe erosion severity classes, respectively. Similarly, about 116.1 and 403.9 ha severe and very severe erosion severity classes remained unchanged, respectively (Table 8).

The mean soil loss in the Chimbel watershed was 24.4 t ha^{-1} year^{-1} in 1989 which increased to 28.3 t ha^{-1} year^{-1} in 2019. The estimated mean annual soil erosion rates in both periods in the watershed study are far beyond the tolerable

Table 8 Soil erosion class change matrix between 1989 and 2019 (area in ha)

Soil erosion severity class in 1989	Soil erosion severity class in 2019 Very slight	Slight	Moderate	Severe	Very severe	Total
Very slight	**1231.2**	125.1	107.5	92.8	190.4	1747.0
Slight	131.2	**141.2**	61.4	66.9	66.4	467.0
Moderate	76.2	38.9	**97.4**	40.0	62.2	314.7
Severe	97.6	57.7	30.6	**116.1**	105.5	407.4
Very severe	168.2	36.5	82.8	77.4	**403.9**	768.9
Total	1704.3	399.4	379.6	393.3	828.5	3705.1

The bold diagonal values are indicating the unchanged land use/land cover and soil erosion respectively

Table 9 The area coverage and soil erosion rates of each LULC types in 1989 and 2019 periods

LULC class	Area (ha)		Mean annual soil loss (t ha^{-1} year^{-1})		Total soil loss (t year^{-1})	
	1989	2019	1989	2019	1989	2019
Bush/shrub land	709	529.2	11.3	11.5	8011.7	6101.7
Grassland	969.2	715	21.5	21.6	20,787.2	15,408.3
Built-up area	108.9	366.5	24.8	25.8	2697.5	9444.7
Forest land	299.7	64.3	8.2	8.3	2463.8	531.8
Cultivated land	1603.8	2022.6	35.3	36.3	56,627.0	73,436.6
Water body	14.5	7.6	–	–	–	–
Total	3705.2	3705.2	24.4	28.3	90,587.2	104,923.0

soil loss rates (i.e., 1–6 t ha^{-1} year^{-1}) (Hurni 1983). Our estimation was consistent with a comprehensive study by Haregeweyn et al. (2017), in the Upper Blue Nile Basin, which found comparable results with an average soil loss rate of 27.54 t ha^{-1} year^{-1}. Similarly, a study conducted in the Guder watershed reported an average soil erosion rate ranging between 25 and 304 t ha^{-1} year^{-1}(Kidane et al. 2019). The result of the soil erosion risk analysis reveals that about 31% of the study area has experienced a soil loss rate higher than the average soil loss tolerance (SLT) adapted to the northwestern highland of Ethiopia. As confirmed from the result, the estimated total soil loss of watershed increases from 90,587.2 t year^{-1} in 1989 to 104,923 t year^{-1} in 2019 (Table 9). The main reason for this increase in soil erosion risk over the study period was attributed to the expansion of cultivated and built-up areas at expense of vegetation covers.

The mean annual soil erosion rates of each LULC category were estimated and the results are indicated in Table 9. The result shows that there is a significant variation between LULC in soil erosion rates. Cultivated land experienced the highest soil loss rates that range from 35.3 t ha^{-1} year^{-1} in 1989 to 36.3 t ha^{-1} year^{-1} in 2019. Similarly, there was an increase in soil erosion rates in the built-up area from 24.8 t ha^{-1} year^{-1} in 1989 to 25.8 t ha^{-1} year^{-1} in 2019. Conversely, the lowest soil loss was observed in forest land, which is 8.2 t ha^{-1} year^{-1} in 1989 and 8.3 t ha^{-1} year^{-1}in 2019. Also, the estimated soil loss rates from grazing land are relatively small, which is 11.2 t ha^{-1} year^{-1} and 11.3 t ha^{-1} year^{-1} in 2019 (Table 9). Studies are also indicated that soil erosion was significantly higher in cultivated land than forest land (Prasannakumar et al. 2012; Kayet et al. 2018; Mukanov et al. 2019).

4 Conclusions

Geospatial technologies and the RUSLE model were integrated to evaluate the effects of LULC changes on water-borne soil erosion. The result reveals that grassland (6.9%),

forest (6.4%), bush/shrubland (4.9%), and water body (0.2%) were reduced, while cultivated land and built-up area increased by 11.3 and 7%, respectively, between 1989 and 2019. Based on the soil erosion severity classes, about 13% of the area was under slight risk, 8.3% was of moderate risk, 11% was a severe risk, and 21% was under very severe erosion risk class in 1989. In 2019, about 46.8% was affected by very slight erosion risk, 12% was of slight erosion risk, 11% was of moderate erosion risk, 8% was affected by severe erosion risk, and 23% of the area was covered by very severe erosion risk. Thus, the result shows an increasing trend in moderate and very severe erosion risk, while very slight and slight erosion risk shows a decreased trend between 1989 and 2019. It was mainly an expansion of cultivated land at the expense of vegetation-covered areas. The mean annual soil erosion from the entire watershed was 24.4 t ha^{-1} year^{-1}in 1989 and 28.3 t ha^{-1} year^{-1} in 2019, which is far beyond the estimated tolerable soil loss (1–6 t ha^{-1} year^{-1}) and soil formation (10–14 t ha^{-1} year^{-1}) rates of the Ethiopian highlands. Cultivated land experienced the highest soil loss rates of 35.3 t ha^{-1} year^{-1}in 1989 and 36.3 t ha^{-1} year^{-1}in 2019. In contrast, the lowest soil loss was observed in forest land which is 8.2 t ha^{-1} year^{-1}in 1989 to 8.3 t ha^{-1} year^{-1} in 2019. Thus, it is important to implement appropriate land management interventions to reverse the trends of LULC changes and soil erosion in the study watershed.

Availability of Data and Materials All the data important for the study are given in the form of figures and tables. However, if the raw data are needed, they can be shared upon request from the corresponding author.

Declarations

Conflict of Interest The authors do not have any competing interest that influences the study.

Ethics Approval and Consent to Participate Not applicable.

Consent for Publication Not applicable.

References

Alexakis DD, Hadjimitsis DG, Agapiou A (2013) Integrated use of remote sensing, GIS and precipitation data for the assessment of soil erosion rate in the catchment area of 'Yialias' in Cyprus. Atmos Res 131:108–124. https://doi.org/10.1016/j.atmosres.2013.02.013

Aneseyee AB, Elias E, Soromessa T, Feyisa GL (2020) Land use/land cover change effect on soil erosion and sediment delivery in the Winike watershed, Omo Gibe Basin, Ethiopia. Sci Total Environ 728:138776. https://doi.org/10.1016/j.scitotenv.2020.138776

Arnoldus HMJ, de Boodt M, Gabriels D (1980) An approximation of the rainfall factor in the Universal Soil Loss Equation. Assess Erosion 6:127–132 (**record number.19831974087**)

Belay T, Mengistu DA (2019) Land use and land cover dynamics and drivers in the Muga watershed, Upper Blue Nile basin, Ethiopia. Remote Sens Appl Soc Envir 15:100249. https://doi.org/10.1016/j.rsase.2019.100249

Belayneh M, Yirgu T, Tsegaye D (2019) Potential soil erosion estimation and area prioritization for better conservation planning in Gumara watershed using RUSLE and GIS techniques'. Environ Syst Res 8:20. https://doi.org/10.1186/s40068-019-0149-x

Benavidez R, Jackson B, Maxwell D, Norton K (2018) A review of the (Revised) Universal Soil Loss Equation ((R)USLE): With a view to increasing its global applicability and improving soil loss estimates. Hydrol Earth Syst Sci 22:6059–6086. https://doi.org/10.5194/hess-22-6059-2018

Bewket W, Abebe S (2013) Land-use and land-cover change and its environmental implications in a tropical highland watershed, Ethiopia. Int J Environ Stud 70(1):126–139. https://doi.org/10.1080/00207233.2012.755765

Demirci A, Karaburun A (2012) Estimation of soil erosion using RUSLE in a GIS framework: a case study in the Buyukcekmece Lake watershed, northwest Turkey. Environ Earth Sci 66(3):903–913. https://doi.org/10.1007/s12665-011-1300-9

Ehsan MA, Tippett MK, Robertson AW, Almazroui M, Ismail M, Dinku T, Acharya N, Siebert A, Ahmed JS, Teshome A (2021) Seasonal predictability of Ethiopian Kiremt rainfall and forecast skill of ECMWF's SEAS5 model. Clim Dyn. https://doi.org/10.1007/s00382-021-05855-0

Esa E, Assen M, Legass A (2018) Implications of land use/cover dynamics on soil erosion potential of agricultural watershed, northwestern highlands of Ethiopia. Environ Syst Res 7(1):21. https://doi.org/10.1186/s40068-018-0122-0

Fenta AA, Yasuda H, Shimizu K, Haregeweyn N, Negussie A (2016) Dynamics of soil erosion as influenced by watershed management practices: a case study of the Agula Watershed in the Semi-Arid

Highlands of Northern Ethiopia. Environ Manag 58:889–905. https://doi.org/10.1007/s00267-016-0757-4

Foody GM (2002) Status of land cover classification accuracy assessment. Remote Sens Environ 80(1):185–201. https://doi.org/10.1016/s0034-4257(01)00295-4

Foody G (2010) Assessing the accuracy of remotely sensed data: principles and practices. Photogram Rec 25(130):204–205. https://doi.org/10.1111/j.1477-9730.2010.00574_2.x

Gao J, Liu Y (2010) Determination of land degradation causes in Tongyu County, Northeast China via land cover change detection. Int J Appl Earth Obs Geoinf 12:9–16. https://doi.org/10.1016/j.jag.2009.08.003

Gashaw T, Tulu T, Argaw M, Worqlul AW (2017) Evaluation and prediction of land use/land cover changes in the Andassa watershed, Blue Nile Basin, Ethiopia. Environ Syst Res 6:17. https://doi.org/10.1186/s40068-017-0094-5

Gashaw T, Tulu T, Argaw M, Worqlul AW (2019) Modeling the impacts of land use—land cover changes on soil erosion and sediment yield in the Andassa watershed, upper Blue Nile basin. Environ Earth Sci 78:679. https://doi.org/10.1007/s12665-019-8726-x

Gashaw T, Worqlul AW, Dile YT, Addisu S, Bantider A, Zeleke G (2020) Evaluating potential impacts of land management practices on soil erosion in the Gilgel Abay watershed, upper Blue Nile basin. Heliyon 6(8):e04777. https://doi.org/10.1016/j.heliyon.2020.e04777

Gebrehiwot SG, Bewket W, Gärdenäs AI, Bishop K (2014) Forest cover change over four decades in the Blue Nile Basin, Ethiopia: Comparison of three watersheds. Reg Environ Change 14:253–266. https://doi.org/10.1007/s10113-013-0483-x

Garede NM, Minale AS (2014) Land use/cover dynamics in ribb watershed, North Western Ethiopia. J Nat Sci Re 4(16):9–16. ISSN : 2224-3186

Haregeweyn N, Tsunekawa A, Poesen J, Tsubo M, Meshesha DT, Fenta AA, Nyssen J, Adgo E (2017) Comprehensive assessment of soil erosion risk for better land use planning in river basins: Case study of the Upper Blue Nile River. Sci Total Environ 574:95–108. https://doi.org/10.1016/j.scitotenv.2016.09.019

Hengl T, De Jesus JM, Heuvelink GBM, Gonzalez MR, Kilibarda M, Blagotić A, Shangguan W, Wright MN, Geng X, Bauer-Marschallinger B, Guevara MA, Vargas R, MacMillan RA, Batjes NH, Leenaars JGB, Ribeiro E, Wheeler I, Mantel S, Kempen B (2017) SoilGrids250m: global gridded soil information based on machine learning. PLoS One 12:e0169748

Hurni H (1983) Soil formation rates in Ethiopia (highlands)—Ethiopian highlands reclamation study. FAO

Hurni H (1985) Erosion–productivity–conservation systems in Ethiopia. In: IV International Conference on Soil Conservation November 3–9, 1985 Maracay, Venezuela, pp 654–674

Kalambukattu J, Kumar S (2017) Modelling soil erosion risk in a mountainous watershed of Mid-Himalaya by integrating RUSLE model with GIS. Euras J Soil Sci. https://doi.org/10.18393/ejss.2017.2.092-105

Karltun E, Lemenih M, Tolera M (2013) Comparing farmers' perception of soil fertility change with soil properties and crop performance in beseku, ethiopia. Land Degrad Dev 24(3):228–235. https://doi.org/10.1002/ldr.1118

Kayet N, Pathak K, Chakrabarty A, Sahoo S (2018) Evaluation of soil loss estimation using the RUSLE model and SCS-CN method in hillslope mining areas. Int Soil Water Conserv Res 6(1):31–42. https://doi.org/10.1016/j.iswcr.2017.11.002

Kidane M, Bezie A, Kesete N, Tolessa T (2019) The impact of land use and land cover (LULC) dynamics on soil erosion and sediment yield in Ethiopia. Heliyon 5(12):e02981. https://doi.org/10.1016/j.heliyon.2019.e02981

Lillesand TM & Kiefer RW (1979) Remote Sensing and Image Interpretation. xii 612 pp, numerous illustrations. New York, Chichester:

John Wiley. ISBN 0471 02609 3. Geological Magazine, 117(3):305-306.https://doi.org/10.1017/S0016756800030636

Mekuriaw A (2017) Assessing the effectiveness of land resource management practices on erosion and vegetative cover using GIS and remote sensing techniques in Melaka watershed. Environ Syst Res 6(16):1–10. https://doi.org/10.1186/s40068-017-0093-6

Meshesha DT, Tsunekawa A, Tsubo M, Haregeweyn N (2012) Dynamics and hotspots of soil erosion and management scenarios of the Central Rift Valley of Ethiopia. Int J Sediment Res 27(1):84–99. https://doi.org/10.1016/s1001-6279(12)60018-3

Mirakhorlo MS, Rahimzadegan M (2020) Evaluating estimated sediment delivery by Revised Universal Soil Loss Equation (RUSLE) and Sediment Delivery Distributed (SEDD) in the Talar Watershed, Iran. Front Earth Sci 14:50–62. https://doi.org/10.1007/s11707-019-0774-8

Moges DM, Bhat HG (2017) Integration of geospatial technologies with RUSLE for analysis of land use/cover change impact on soil erosion: case study in Rib watershed, north-western highland Ethiopia. Environ Earth Sci 76:765. https://doi.org/10.1007/s12665-017-7109-4

Moore ID, Burch GJ (1986) Physical basis of the length-slope factor in the universal soil loss equation. Soil Sci Soc Am J 50(5):1294. https://doi.org/10.2136/sssaj1986.03615995005

Mukanov Y, Chen Y, Baisholanov S, Amanambu AC, Issanova G, Abenova A, Fang G, Abayev N (2019) Estimation of annual average soil loss using the Revised Universal Soil Loss Equation (RUSLE) integrated in a Geographical Information System (GIS) of the Esil River basin (ERB), Kazakhstan. Acta Geophys 67:921–938

Negese A (2021) Impacts of land use and land cover change on soil erosion and hydrological responses in Ethiopia. Appl Environ Soil Sci 2021:10

Phinzi K, Ngetar NS (2019) The assessment of water-borne erosion at catchment level using GIS-based RUSLE and remote sensing: a review. Int Soil Water Conserv Res 7:27–46. https://doi.org/10.1016/j.iswcr.2018.12.002

Prasannakumar V, Vijith H, Abinod S, Geetha N (2012) Estimation of soil erosion risk within a small mountainous sub-watershed in Kerala, India, using Revised Universal Soil Loss Equation (RUSLE) and geo-information technology. Geosci Front 3(2):209–215. https://doi.org/10.1016/j.gsf.2011.11.003

Shalaby A, Tateishi R (2007) Remote sensing and GIS for mapping and monitoring land cover and land-use changes in the Northwestern coastal zone of Egypt. Appl Geogr 27(1):28–41. https://doi.org/10.1016/j.apgeog.2006.09.004

Tamene L, Vlek PLG (2008) Soil erosion studies in Northern Ethiopia. In: Braimoh AK, Vlek PLG (eds) Land use and soil resources. Springer, Dordrecht. https://doi.org/10.1007/978-1-4020-6778-5_5

Tebebu TY, Abiy AZ, Zegeye AD, Dahlke HE, Easton ZM, Tilahun SA, Collick AS, Kidnau S, Moges S, Dadgari F, Steenhuis TS (2010) Surface and subsurface flow effect on permanent gully formation and upland erosion near Lake Tana in the northern highlands of Ethiopia. Hydrol Earth Syst Sci 14:2207–2217. https://doi.org/10.5194/hessd-7-5235-2010

Teferi E, Bewket W, Uhlenbrook S, Wenninger J (2013) Understanding recent land use and land cover dynamics in the source region of the Upper Blue Nile, Ethiopia: spatially explicit statistical modeling of systematic transitions. Agric Ecosyst Environ 165:98–117. https://doi.org/10.1016/j.agee.2012.11.007

Tolessa T, Senbeta F, Kidane M (2017) The impact of land use/land cover change on ecosystem services in the central highlands of Ethiopia. Ecosyst Serv 23:47–54. https://doi.org/10.1016/j.ecoser.2016.11.010

Wischmeier W, Smith D (1978) Predicting rainfall erosion losses: a guide to conservation planning. U.S. Department of Agriculture Handbook No. 537

Woldemariam GW, Harka AE (2020) Effect of land use and land cover change on soil erosion in erer sub-basin, Northeast Wabi Shebelle Basin, Ethiopia. Land 9:111. https://doi.org/10.3390/land9040111

Wolka K, Tadesse H, Garedew E, Yimer F (2015) Soil erosion risk assessment in the Chaleleka wetland watershed, Central Rift Valley of Ethiopia. Environ Syst Res 4:5. https://doi.org/10.1186/s40068-015-0030-5

Zerihun M, Mohammedyasin MS, Sewnet D, Adem AA, Lakew M (2018) Assessment of soil erosion using RUSLE, GIS and remote sensing in NW Ethiopia. Geodrs 12:83–90. https://doi.org/10.1016/j.geodrs.2018.01.002

Zhu Z, Woodcock CE (2014) Continuous change detection and classification of land cover using all available Landsat data. Remote Sens Environ 144:152–171. https://doi.org/10.1016/j.rse.2014.01.011